Sally K. Martin, Stephen Fitter, Ankit K. Dutta, Mary P. Matthews,Carl R. Walkley, Michael N. Hall, Markus A. Ruegg, Stan Gronthos, Andrew C. W. Zannettino

Brief report: The differential roles of mTORC1 and mTORC2 in mesenchymal stem cell differentiation

Stem Cells, 2015; 33(4):1359-1365

The differential roles of mTORC1 and mTORC2 in mesenchymal stem cell differentiation.

Sally K. Martin[1,2,3], Stephen Fitter[1,2,3], Ankit K. Dutta[1], Mary P. Matthews[1], Carl R. Walkley[4], Michael N. Hall[5], Markus A. Ruegg[5], Stan Gronthos[3,6], Andrew C.W. Zannettino[1,2,3]

[1]Myeloma Research Laboratory, School of Medical Sciences, University of Adelaide, Australia; [2]Centre for Cancer Biology, SA Pathology, Australia; [3]Centre for Stem Cell Research, University of Adelaide, Australia; [4]Stem Cell Regulation Laboratory, St Vincent's Institute, Melbourne, Australia; [5]Biozeutrum, University of Basel, Switzerland; [6]Mesenchymal Stem Cell Laboratory, School of Medical Sciences, University of Adelaide, Australia.

Running title: The Role of mTORC1 and mTORC2 in MSC Differentiation.

Keywords: mesenchymal stem cell, mTOR, raptor, rictor

Author contributions: Conceived and designed the experiments: SKM, SF, ACWZ. Performed the experiments: SKM, SF, AKD, MPM. Analysed the data: SKM, SF, AKD, MEM. Contributed reagents, expertise and materials: CRW, MAR, MNH, SG. Wrote the paper: SKM. All authors were involved in the final approval of this manuscript.

Corresponding Author: Dr Sally Martin, Myeloma Research Laboratory, South Australian Health and Medical Research Institute (SAHMRI), PO Box 11060, Adelaide, South Australia, 5001, AUSTRALIA. Phone: +61 8 8128 4694. E-mail: sally.martin@adelaide.edu.au

ABSTRACT

Adipocytes (AdCs) and osteoblasts (OBs) are derived from mesenchymal stem cells (MSCs) and differentiation toward either lineage is both mutually exclusive and transcriptionally controlled. Recent studies implicate the mammalian target of rapamycin (mTOR) pathway as important in determining MSC fate, with inhibition of mTOR promoting OB differentiation and suppressing AdC differentiation. mTOR functions within two distinct multiprotein complexes, mTORC1 and mTORC2, each of which contains the unique adaptor protein, raptor or rictor, respectively. While compounds used to study mTOR signalling, such as rapamycin and related analogues, primarily inhibit mTORC1, prolonged exposure can also disrupt mTORC2 function, confounding interpretation of inhibitor studies. As a result, the relative contribution of mTORC1 and mTORC2 to MSC fate determination remains unclear.

In this study, we generated primary mouse MSCs deficient in either *Rptor* (RapKO) or *Rictor* (RicKO) using the Cre/*loxP* system. Cre-mediated deletion of *Rptor* or *Rictor* resulted in impaired mTORC1 and mTORC2 signalling, respectively. Under lineage-inductive culture conditions, RapKO MSC displayed a reduced capacity to form lipid-laden AdCs and an increased capacity to form a mineralised matrix. In contrast, RicKO MSC displayed reduced osteogenic differentiation capacity and enhanced adipogenic differentiation potential. Taken together, our findings reveal distinct roles for mTORC1 and mTORC2 in lineage commitment of MSCs.

INTRODUCTION

Mesenchymal stem cells (MSCs) are multipotent progenitor cells that, in response to extracellular factors and environmental cues, differentiate into several specialised cell types including adipocytes (AdCs) and osteoblasts (OBs). *In vitro*, lineage specification can be guided by inductive culture conditions. Murine MSC cultures stimulated with glucocorticoid, insulin and indomethacin differentiate into mature lipid-laden AdCs, whereas cultures supplemented with a source of inorganic phosphate and glucocorticoid differentiate into mineralised matrix-producing OBs.

Several signalling pathways have been shown to regulate MSC differentiation *in vitro* **(1-5)**. The mammalian target of rapamycin (mTOR) pathway is the primary nutrient-sensing pathway that controls cell growth and metabolism. mTOR plays an important role in the adipogenic program, as rapamycin, an allosteric mTOR inhibitor, inhibits adipogenesis **(6-10)** whilst deletion of TSC2, a negative regulator of mTOR, promotes adipogenesis **(10)**.

The role of mTOR in MSC commitment to other lineages is less clear. Most notably, rapamycin studies have shown to have both inhibitory **(11-16)** and stimulatory **(17-20)** effects on osteogenesis, a disparity which may reflect the nature of the target cells used. Furthermore, rapamycin sequesters FKBP12 **(21)**, a negative regulator of TGFβ1 signalling, and thus the pro-osteogenic effects of rapamycin may be the indirect result of TGFβ1 activation.

mTOR exists in two distinct complexes, mTORC1 and mTORC2, each of which is defined by the unique adaptor proteins raptor and rictor, respectively. mTORC1 controls protein synthesis, ribosome biogenesis and nutrient transport **(22,23)** whereas mTORC2 regulates cell survival, metabolism and cytoskeletal organisation **(24)**. While rapamycin primarily inhibits mTORC1, prolonged exposure can also disrupt mTORC2 function **(25,26)**,

confounding data interpretation with respect to MSC differentiation and the role played by mTORC1 and mTORC2 in osteogenesis.

In the current study we utilised a genetic approach to specifically delete *Rptor* or *Rictor* in primary MSCs and examine the roles of mTORC1 and mTORC2 in osteogenic and adipogenic MSC differentiation.

RESULTS

Generation of Rptor and Rictor knockout MSCs. Primary compact bone-derived MSCs were isolated from $Rptor^{fl/fl}$ or $Rictor^{fl/fl}$ mice, and infected with a tamoxifen-inducible self-deleting Cre recombinase ($CreER^{T2}$) or empty vector as a control. Tamoxifen **(**4-OHT) treatment induced the nuclear translocation of $CreER^{T2}$, resulting in *Rptor* or *Rictor* deficient MSCs, termed RapKO and RicKO, respectively (Fig. 1A).

Protein levels of RPTOR and RICTOR and the activation status of mTORC1 and mTORC2 downstream effectors was assessed by western immunoblotting. As previously reported **(27-29)**, low levels of residual RPTOR or RICTOR protein expression in RapKO and RicKO cells were observed (Fig. 1B). Consistent with disruption of mTORC1 function, *Rptor* deletion resulted in decreased S6K phosphorylation, and hyperphosphorylation of Akt_{Thr308}, IRS-1 and FOXO1/3a (Fig. 1B). *Rictor* deletion resulted in ablation of Akt_{Ser473} phosphorylation, in keeping with mTORC2 substrate specificity (Fig. 1B).

Loss of Rptor, but not Rictor, impairs MSC proliferation. The effect of *Rptor* or *Rictor* knockout on MSC growth was examined using WST-1 and BrdU assays. RapKO cells displayed a significant decrease in growth after 3, 5 and 7 days compared to controls (Fig. 1C). In contrast, no difference in proliferation was observed in response to *Rictor* deletion (Fig. 1D).

To determine whether the inhibition of RapKO cell proliferation was associated with an induction of apoptosis, RapKO and control MSCs were stained with Annexin V and 7-AAD. Whilst no significant difference in Annexin V labelling was observed, a 2-fold increase in 7-AAD positive cells was evident in RapKO MSCs compared to controls (Fig. 1E).

The roles of Rptor and Rictor in osteogenic and adipogenic MSC differentiation. We next examined the ability of RapKO and RicKO cells to differentiate into mature OBs and form a mineralised extracellular matrix **(30,31)**. Under osteoinductive conditions, RapKO cells displayed a 5-fold increase in mineral formation relative to controls (Fig. 2A), whereas RicKO cells displayed a 2-fold decrease in mineral formation (Fig. 2B).

In parallel experiments, the potential of RapKO, RicKO and control MSCs to differentiate into functional AdCs was also assessed. Quantitation of lipid-laden, Nile Red-stained adipocytes, relative to total cell number, showed that deletion of *Rptor* induced a 1.8-fold decrease in AdC formation, whereas deletion of *Rictor* resulted in a 1.8-fold increase in AdC formation (Fig. 2C and Fig. 2D).

Loss of Rptor promotes osteogenesis and inhibits adipogenesis. To gain insight into the molecular mechanisms by which *Rptor* deletion promotes osteogenic MSC differentiation, temporal gene expression analyses were performed. Loss of *Rptor* induced a strong up-regulation of genes involved in OB differentiation including the osteogenic transcription factors Cbfa-1 (*Runx2*) and osterix (*Sp7*), and the marker of OB function, alkaline phosphatase (*Alpl*) (Fig. 3A). In inductive differentiation media, *Rptor* deletion was also associated with an increase in the expression of BMP-2 and other osteogenic TGFβ superfamily members such as inhibinβ A chain (*Inhba*) and inhibinβ E chain (*Inhbe*). In contrast, expression of integrin binding sialoprotein (*Ibsp*) was strongly down-regulated in RapKO cultures, as was the expression of noggin (*Nog*), a negative regulator of BMP signalling (Fig. 3A).

In parallel experiments, the effect of *Rptor* deletion on molecular markers of AdC differentiation and function was also examined. Consistent with the marked inhibition of AdC formation in RapKO MSCs (Fig. 2C), the expression of *Cebpa* and *Pparg,* transcription factors essential for adipogenesis, and adiponectin (*Adipoq*), a marker of mature adipocytes, was down-regulated in RapKO MSCs at all time points examined (Fig. 3B).

Loss of Rictor promotes adipogenesis and inhibits osteogenesis. We also examined the temporal regulation of adipogenic genes in RicKO and control MSCs during adipogenic differentiation. Consistent with the induction of AdC formation in RicKO MSCs (Fig 2D), the expression of *Cebpa*, *Pparγ* and *Adipoq* was strongly up-regulated in RicKO MSCs at all time points examined (Fig. 4A). Under osteoinductive culture conditions, loss of *Rictor* was associated with a down-regulation of *Runx2*, *Sp7*, *Alpl, Bmp2* and *Inhba* expression (Fig. 4B), consistent with the inhibition of osteogenesis observed in RicKO cells (Fig. 2B).

DISCUSSION

Using Cre-mediated gene deletion and well-established *in vitro* differentiation assays, we have shown that mTORC1 and mTORC2 have distinct roles in MSC fate determination. Consistent with previous studies (reviewed in **(32)**), deletion of *Rptor* in MSCs reduced their adipogenic potential. Under osteoinductive conditions however, *Rptor* deletion promoted osteogenic differentiation. This switching between differentiation programs could reflect the mutual exclusivity of these programs (i.e. enhanced osteogenesis in the absence of mTORC1-mediated PPARγ activation). Alternatively, loss of mTORC1 may maintain the osteogenic potential of MSCs, in line with studies showing that rapamycin attenuates stem cell aging, maintaining their self-renewal and osteogenic potential **(33-36)**, and with *in vivo* studies showing that deletion of p70S6K (mTORC1 effector) protects against age-related bone loss **(37)**.

While further studies are required to characterise the precise mechanism(s) by which mTORC1 inhibition promotes osteogenesis, our PCR data suggests that BMP signalling is involved. Many BMPs are strongly pro-osteogenic (reviewed in **(38)**), however their role in osteogenesis is complex **(39,40)**, influenced by variables such as dose **(41)** and BMP receptor subtype **(39,42)**.

In contrast to RapKO cells, *Rictor* deletion promoted adipogenesis and inhibited osteogenesis, which is consistent with a recent siRNA study which showed that mTORC2 regulation of cytoskeletal organisation plays a role in MSC fate determination in response to mechanical stress **(43)**. These findings suggest that the decreased osteogenic potential of RicKO cells may be associated with impaired cytoskeletal organisation.

Overall, these findings provide new insight into the role of mTOR signalling in MSC lineage commitment.

ACKNOWLEDGEMENTS

The authors thank Dr Kristoffer Riecken (University Medical Centre Hamburg) for the LeGO-iG2 vector and Dr Pierre Chambon (IGBMC, France) for the Cre-ER^{T2} expression vector. This work was supported by grants awarded by the National Health and Medical Research Council of Australia (APP1030528), a Royal Adelaide Hospital Mary Overton Early Career Fellowship (SKM) and an Australian Postgraduate Award (MPM). The authors gratefully acknowledge the assistance of Kate Pilkington and Rebecca Salmon (Detmold Family Imaging Facility, SA Pathology) with cell sorting.

REFERENCES

1. Rodda SJ, McMahon AP 2006 Distinct roles for Hedgehog and canonical Wnt signaling in specification, differentiation and maintenance of osteoblast progenitors. Development **133**(16)**:**3231-44.
2. Hu H, Hilton MJ, Tu X, Yu K, Ornitz DM, Long F 2005 Sequential roles of Hedgehog and Wnt signaling in osteoblast development. Development **132**(1)**:**49-60.
3. Kang S, Bennett CN, Gerin I, Rapp LA, Hankenson KD, Macdougald OA 2007 Wnt signaling stimulates osteoblastogenesis of mesenchymal precursors by suppressing CCAAT/enhancer-binding protein alpha and peroxisome proliferator-activated receptor gamma. J Biol Chem **282**(19)**:**14515-24.
4. Long F, Chung UI, Ohba S, McMahon J, Kronenberg HM, McMahon AP 2004 Ihh signaling is directly required for the osteoblast lineage in the endochondral skeleton. Development **131**(6)**:**1309-18.
5. Nakae J, Kitamura T, Kitamura Y, Biggs WH, 3rd, Arden KC, Accili D 2003 The forkhead transcription factor Foxo1 regulates adipocyte differentiation. Dev Cell **4**(1)**:**119-29.
6. Bell A, Grunder L, Sorisky A 2000 Rapamycin inhibits human adipocyte differentiation in primary culture. Obes Res **8**(3)**:**249-54.
7. Cho HJ, Park J, Lee HW, Lee YS, Kim JB 2004 Regulation of adipocyte differentiation and insulin action with rapamycin. Biochem Biophys Res Commun **321**(4)**:**942-8.
8. El-Chaar D, Gagnon A, Sorisky A 2004 Inhibition of insulin signaling and adipogenesis by rapamycin: effect on phosphorylation of p70 S6 kinase vs eIF4E-BP1. Int J Obes Relat Metab Disord **28**(2)**:**191-8.
9. Yeh WC, Bierer BE, McKnight SL 1995 Rapamycin inhibits clonal expansion and adipogenic differentiation of 3T3-L1 cells. Proc Natl Acad Sci U S A **92**(24)**:**11086-90.
10. Zhang HH, Huang J, Duvel K, Boback B, Wu S, Squillace RM, Wu CL, Manning BD 2009 Insulin stimulates adipogenesis through the Akt-TSC2-mTORC1 pathway. PLoS ONE **4**(7)**:**e6189.
11. Isomoto S, Hattori K, Ohgushi H, Nakajima H, Tanaka Y, Takakura Y 2007 Rapamycin as an inhibitor of osteogenic differentiation in bone marrow-derived mesenchymal stem cells. J Orthop Sci **12**(1)**:**83-8.
12. Singha UK, Jiang Y, Yu S, Luo M, Lu Y, Zhang J, Xiao G 2008 Rapamycin inhibits osteoblast proliferation and differentiation in MC3T3-E1 cells and primary mouse bone marrow stromal cells. J Cell Biochem **103**(2)**:**434-46.
13. Tang L, Ebara S, Kawasaki S, Wakabayashi S, Nikaido T, Takaoka K 2002 FK506 enhanced osteoblastic differentiation in mesenchymal cells. Cell Biol Int **26**(1)**:**75-84.
14. Shoba LN, Lee JC 2003 Inhibition of phosphatidylinositol 3-kinase and p70S6 kinase blocks osteogenic protein-1 induction of alkaline phosphatase activity in fetal rat calvaria cells. J Cell Biochem **88**(6)**:**1247-55.
15. Phornphutkul C, Lee M, Voigt C, Wu KY, Ehrlich MG, Gruppuso PA, Chen Q 2009 The effect of rapamycin on bone growth in rabbits. J Orthop Res.
16. Alvarez-Garcia O, Carbajo-Perez E, Garcia E, Gil H, Molinos I, Rodriguez J, Ordonez FA, Santos F 2007 Rapamycin retards growth and causes marked alterations in the growth plate of young rats. Pediatr Nephrol **22**(7)**:**954-61.
17. Vinals F, Lopez-Rovira T, Rosa JL, Ventura F 2002 Inhibition of PI3K/p70 S6K and p38 MAPK cascades increases osteoblastic differentiation induced by BMP-2. FEBS Lett **510**(1-2)**:**99-104.

18. Lee KW, Yook JY, Son MY, Kim MJ, Koo DB, Han YM, Cho YS 2010 Rapamycin promotes the osteoblastic differentiation of human embryonic stem cells by blocking the mTOR pathway and stimulating the BMP/Smad pathway. Stem Cells Dev **19**(4)**:**557-68.
19. Ogawa T, Tokuda M, Tomizawa K, Matsui H, Itano T, Konishi R, Nagahata S, Hatase O 1998 Osteoblastic differentiation is enhanced by rapamycin in rat osteoblast-like osteosarcoma (ROS 17/2.8) cells. Biochem Biophys Res Commun **249**(1)**:**226-30.
20. Martin SK, Fitter S, Bong LF, Drew JJ, Gronthos S, Shepherd PR, Zannettino AC 2010 NVP-BEZ235, a dual pan class I PI3 kinase and mTOR inhibitor, promotes osteogenic differentiation in human mesenchymal stromal cells. J Bone Miner Res **25**(10)**:**2126-37.
21. Chen YG, Liu F, Massague J 1997 Mechanism of TGFbeta receptor inhibition by FKBP12. Embo J **16**(13)**:**3866-76.
22. Kim DH, Sarbassov DD, Ali SM, King JE, Latek RR, Erdjument-Bromage H, Tempst P, Sabatini DM 2002 mTOR interacts with raptor to form a nutrient-sensitive complex that signals to the cell growth machinery. Cell **110**(2)**:**163-75.
23. Kim DH, Sarbassov DD, Ali SM, Latek RR, Guntur KV, Erdjument-Bromage H, Tempst P, Sabatini DM 2003 GbetaL, a positive regulator of the rapamycin-sensitive pathway required for the nutrient-sensitive interaction between raptor and mTOR. Mol Cell **11**(4)**:**895-904.
24. Laplante M, Sabatini DM 2012 mTOR signaling in growth control and disease. Cell **149**(2)**:**274-93.
25. Lamming DW, Ye L, Katajisto P, Goncalves MD, Saitoh M, Stevens DM, Davis JG, Salmon AB, Richardson A, Ahima RS, Guertin DA, Sabatini DM, Baur JA 2012 Rapamycin-induced insulin resistance is mediated by mTORC2 loss and uncoupled from longevity. Science **335**(6076)**:**1638-43.
26. Sarbassov DD, Ali SM, Sengupta S, Sheen JH, Hsu PP, Bagley AF, Markhard AL, Sabatini DM 2006 Prolonged rapamycin treatment inhibits mTORC2 assembly and Akt/PKB. Mol Cell **22**(2)**:**159-68.
27. Cybulski N, Zinzalla V, Hall MN 2012 Inducible raptor and rictor knockout mouse embryonic fibroblasts. Methods Mol Biol **821:**267-78.
28. Patursky-Polischuk I, Stolovich-Rain M, Hausner-Hanochi M, Kasir J, Cybulski N, Avruch J, Ruegg MA, Hall MN, Meyuhas O 2009 The TSC-mTOR pathway mediates translational activation of TOP mRNAs by insulin largely in a raptor- or rictor-independent manner. Mol Cell Biol **29**(3)**:**640-9.
29. Chen J, Long F 2014 mTORC1 signaling controls mammalian skeletal growth through stimulation of protein synthesis. Development **141**(14)**:**2848-54.
30. Gundle R, Stewart K, Screen J, Beresford JN 1998 Isolation and culture of human bone-derived cells. In: Beresford JN, Owen ME (eds.) Marrow stromal cell culture. Cambrige University Press, Cambridge, pp 43-66.
31. Jaiswal N, Haynesworth SE, Caplan AI, Bruder SP 1997 Osteogenic differentiation of purified, culture-expanded human mesenchymal stem cells in vitro. J Cell Biochem **64**(2)**:**295-312.
32. Xiang X, Zhao J, Xu G, Li Y, Zhang W 2011 mTOR and the differentiation of mesenchymal stem cells. Acta Biochim Biophys Sin (Shanghai) **43**(7)**:**501-10.
33. Castilho RM, Squarize CH, Chodosh LA, Williams BO, Gutkind JS 2009 mTOR mediates Wnt-induced epidermal stem cell exhaustion and aging. Cell Stem Cell **5**(3)**:**279-89.

34. Chen C, Liu Y, Zheng P 2009 mTOR regulation and therapeutic rejuvenation of aging hematopoietic stem cells. Sci Signal **2**(98)**:**ra75.
35. Iglesias-Bartolome R, Patel V, Cotrim A, Leelahavanichkul K, Molinolo AA, Mitchell JB, Gutkind JS 2012 mTOR inhibition prevents epithelial stem cell senescence and protects from radiation-induced mucositis. Cell Stem Cell **11**(3)**:**401-14.
36. Gharibi B, Farzadi S, Ghuman M, Hughes FJ 2014 Inhibition of Akt/mTOR attenuates age-related changes in mesenchymal stem cells. Stem Cells **32**(8)**:**2256-66.
37. Selman C, Tullet JM, Wieser D, Irvine E, Lingard SJ, Choudhury AI, Claret M, Al-Qassab H, Carmignac D, Ramadani F, Woods A, Robinson IC, Schuster E, Batterham RL, Kozma SC, Thomas G, Carling D, Okkenhaug K, Thornton JM, Partridge L, Gems D, Withers DJ 2009 Ribosomal protein S6 kinase 1 signaling regulates mammalian life span. Science **326**(5949)**:**140-4.
38. Chen G, Deng C, Li YP 2012 TGF-beta and BMP signaling in osteoblast differentiation and bone formation. Int J Biol Sci **8**(2)**:**272-88.
39. Chen D, Ji X, Harris MA, Feng JQ, Karsenty G, Celeste AJ, Rosen V, Mundy GR, Harris SE 1998 Differential roles for bone morphogenetic protein (BMP) receptor type IB and IA in differentiation and specification of mesenchymal precursor cells to osteoblast and adipocyte lineages. J Cell Biol **142**(1)**:**295-305.
40. Kang Q, Song WX, Luo Q, Tang N, Luo J, Luo X, Chen J, Bi Y, He BC, Park JK, Jiang W, Tang Y, Huang J, Su Y, Zhu GH, He Y, Yin H, Hu Z, Wang Y, Chen L, Zuo GW, Pan X, Shen J, Vokes T, Reid RR, Haydon RC, Luu HH, He TC 2009 A comprehensive analysis of the dual roles of BMPs in regulating adipogenic and osteogenic differentiation of mesenchymal progenitor cells. Stem Cells Dev **18**(4)**:**545-59.
41. Wang EA, Israel DI, Kelly S, Luxenberg DP 1993 Bone morphogenetic protein-2 causes commitment and differentiation in C3H10T1/2 and 3T3 cells. Growth Factors **9**(1)**:**57-71.
42. Liu HY, Wu AT, Tsai CY, Chou KR, Zeng R, Wang MF, Chang WC, Hwang SM, Su CH, Deng WP 2011 The balance between adipogenesis and osteogenesis in bone regeneration by platelet-rich plasma for age-related osteoporosis. Biomaterials **32**(28)**:**6773-80.
43. Sen B, Xie Z, Case N, Thompson WR, Uzer G, Styner M, Rubin J 2014 mTORC2 regulates mechanically induced cytoskeletal reorganization and lineage selection in marrow-derived mesenchymal stem cells. J Bone Miner Res **29**(1)**:**78-89.

FIGURE LEGENDS

Figure 1. Cre-mediated loss of *Rptor* and *Rictor* expression in RapKO and RicKO MSCs. (A) Workflow illustrating the generation of RapKO, RicKO and control MSC lines. **(B)** *Rptor*$^{fl/fl}$ and *Rictor*$^{fl/fl}$ MSCs infected with the CreER^{T2} lentivirus were treated with 4-OHT, to induce *Rptor* or *Rictor* knockout, or vehicle as a control. Lysates were prepared from control, RapKO and RicKO MSCs and western blot analysis performed using antibodies directed against the proteins indicated. **(C, D)** RapKO, RicKO and control MSCs were cultured for 7 days and proliferation assessed using WST-1 and BrdU assays. Both cumulative WST-1 data (left) and BrdU data from the Day 7 time point (right) are shown, expressed as the mean ± SD of quintuplicate wells from a representative experiment of three. **p<0.005, ****p<0.0001, t-test. **(E)** RapKO cells were stained for the apoptotic markers Annexin V and 7-AAD, and analysed immediately by flow cytometry.

Figure 2. Differential roles for *Rptor* and *Rictor* in osteogenic and adipogenic MSC differentiation. *Rptor*$^{fl/fl}$ and *Rictor*$^{fl/fl}$ MSCs infected with the CreER^{T2} lentivirus or empty vector were treated for 8 days with 4-OHT (+) or vehicle (-). **(A, B)** Treated cells were cultured under osteoinductive conditions for 21 days and the amount of acid-solubilised calcium was quantitated and normalised to cell number. Data are expressed as the mean ± SD of quadruplicate wells from a representative experiment of three. Representative images of Alizarin Red-stained wells are shown. **(C, D)** Treated cells were cultured under adipogenic conditions for 8 days. Adipocytes were visualised using Nile Red, and the number of adipocytes quantitated and normalised to total cell number. Data are expressed as the mean ± SD of quadruplicate wells from a representative experiment of three. *p<0.05, **p<0.005, ***p<0.0005, ****p<0.0001, t-test.

Figure 3. Loss of *Rptor* promotes osteogenesis and inhibits adipogenesis. *Raptor*$^{fl/fl}$ MSCs infected with the CreER^{T2} lentivirus were treated with vehicle (control) or 4-OHT (RapKO) for 8 days. **(A)** Treated cells were cultured under osteogenic conditions for 22 days and RNA harvested at the indicated time points. The mRNA level of osteogenic genes was examined by real-time PCR and data were normalised to β-actin. **(B)** Treated cells were cultured under adipogenic conditions for 8 days and RNA harvested at the indicated time points. The mRNA level of adipogenic genes was examined by real-time PCR and data were normalised to β-actin. *p<0.05, **p<0.005, ***p<0.0005, ****p<0.0001, t-test.

Figure 4. Loss of *Rictor* promotes adipogenesis and inhibits osteogenesis. *Rictor*$^{fl/fl}$ MSCs infected with the CreER^{T2} lentivirus were treated with vehicle (control) or 4-OHT (RicKO) for 8 days. **(A)** Treated cells were cultured under adipogenic conditions for 8 days and RNA harvested at the indicated time points. The mRNA level of adipogenic genes was examined by real-time PCR and data were normalised to β-actin. **(B)** Treated cells were cultured under osteogenic conditions for 22 days and RNA harvested at the indicated time points. The mRNA level of osteogenic genes was examined by real-time PCR and data were normalised to β-actin. *p<0.05, **p<0.005, ***p<0.0005, ****p<0.0001, t-test.

MATERIALS AND METHODS

Compact bone MSC isolation. Murine compact bone MSCs (CB MSCs) were derived from the long bones of 6-7 week old *Rptor*$^{fl/fl}$ and *Rictor*$^{fl/fl}$ mice **(1)** according to previously established protocols **(2)**, with approval from SA Pathology/CALHN and University of Adelaide Animal Ethics Committees. Briefly, tibiae and femora from 8-12 mice were excised, cleaned thoroughly with a scalpel and epiphyses removed. The bones were then pooled, crushed in ice-cold PBS supplemented with 2% FCS and 2 mM EDTA, washed several times, chopped into small fragments and digested in 3 mg/mL Type 1 collagenase at 37^{o}C (Worthington Biochemical Corporation, NJ, USA) for 45 minutes on a shaking platform. The resultant cell suspension was filtered through a 70 μm strainer, pelleted by centrifugation and lineage depletion performed using a cocktail of biotinylated antibodies to CD3, CD4, CD5, CD8, CD11b, Gr-1, B220, Ter-119 (BioLegend, CA, USA), followed by a streptavidin-APC conjugate (Invitrogen/ Life Technologies, VIC, Australia). Cells were also stained with CD51-PE, CD31-PerCP Cy5.5 (BioLegend), Sca-1-PeCy7 (BD Biosciences, NJ, USA), CD45-eF780 (eBioscience, CA, USA), and fluorogold (Invitrogen) to exclude non-viable cells. Fluorescence Activated Cell Sorting (FACS) was performed to collect Lin-CD45-CD31-CD51-Sca-1+ cells (FACSAria, Becton Dickinson).

FACS-isolated CB MSCs were cultured in α-MEM supplemented with 20% FCS, 2 mM L-glutamine, 100 μM L-ascorbate-2-phosphate, 50 IU/mL penicillin, 50 μg/mL streptomycin sulphate, 1 mM sodium pyruvate and 15 mM HEPES (Sigma Aldrich, NSW, Australia) in a hypoxic *in vitro* cabinet (5% O_2, 10% CO_2, 85% N_2, Coy Laboratory Products, MI, USA) at 37^{o}C **(2)**. Cells were passaged by detachment with a 0.05% trypsin-EDTA solution upon reaching 80-90% confluence.

Cre-mediated gene deletion. CB MSCs (passages 2-3) were infected with a lentivirus carrying a tamoxifen-inducible self-deleting Cre recombinase (LEGO-CreER^{T2}-iG2), or

empty vector control (LEGO-iG2) **(3)** in the presence of 4 μg/mL polybrene. CB MSCs with stable lentiviral integration were selected on the basis of GFP expression. Following *in vitro* expansion, cells were treated with 0.5 μM 4-hydroxytamoxifen (4-OHT, Sigma Aldrich) for 8 days to induce *Rptor* or *Rictor* deletion. Ethanol (0.05%) was used as a vehicle control. To exclude any 4-OHT-induced effects unrelated to the knockout of *Rptor* or *Rictor*, cells infected with a LEGO-iG2 vector control, were used in all studies.

Mineralisation Assay. CB MSCs ($3.75x10^4$ cells/cm^2) were seeded into quadruplicate wells of a 48-well plate in α-MEM and allowed to adhere overnight. The next day, media were replaced with α-MEM supplemented with 20% FCS, 10^{-8} M dexamethasone sodium phosphate, 100 μM ascorbate-2-phosphate, 4 mM KH_2PO_4 (Asia Pacific Speciality Chemicals, NSW, Australia), and cells were cultured under hypoxic conditions with media changed twice weekly for 22 days. Mineral content was quantified by measuring the concentration of Ca^{2+} in acid-solubilised matrix using the Arsenazo kit (Thermo Scientific, MA, USA), normalised to the number of cells per well using the Quant-iT™ Pico Green dsDNA assay (Invitrogen). To visualise calcium deposits, formalin-fixed cultures were stained with Alizarin Red S (Sigma Aldrich) for 1 hour, rinsed with water and allowed to air-dry.

Adipogenesis Assay. CB MSCs ($3.75x10^4$ cells/cm^2) were seeded into quadruplicate wells of a 48-well plate in α-MEM and allowed to adhere overnight. The next day, media were replaced with α-MEM supplemented with 20% FCS, 10^{-6} M dexamethasone sodium phosphate, 60 μM indomethacin (Sigma Aldrich) and 1 μg/mL insulin (Novo Nordisk, NSW, Australia), and cells were cultured under hypoxic conditions with media changed twice weekly for 8 days. To identify and enumerate lipid-laden fat cells, formalin-fixed cells were stained with 25 ng/mL Nile Red (Sigma Aldrich) and 300 nmol/L DAPI (Invitrogen) for 15 minutes. Nile

Red-labelled adipocytes and DAPI-stained cell nuclei were visualised using an inverted fluorescence microscope (CKX41; Olympus, Japan), and adipocytes and cell nuclei were enumerated from multiple images from each well (10x magnification) using Adobe Photoshop and Image J software, respectively.

Cell Growth (WST-1). MSCs ($1.25x10^4$ cells/cm^2) were seeded into quintuplicate wells of a 96-well plate in α-MEM and allowed to adhere overnight. The number of viable cells present was assessed at the indicated time points using the colorimetric reagent WST-1 as per manufacturers' instructions (Roche, NSW, Australia).

Cell Growth (BrdU). MSCs ($1.25x10^4$ cells/cm^2) were seeded into quintuplicate wells of a 96-well plate in α-MEM. The number of viable cells present after 7 days was assessed by incubating cells with 5-bromo-2'-deoxyuridine (BrdU) for 16 hours and then detecting the incorporated BrdU using a colorimetric assay as per manufacturer's instructions (Roche).

Apoptosis. CB MSCs were stained with 5 uL Annexin V-PECy7 (eBioscience) and 20 uL 7-Aminoactinomycin (7-AAD, Invitrogen) for 15 minutes as per manufacturers' instructions, and analysed immediately by flow cytometry (FC-500, Beckman Coulter, CA, USA). Cells incubated in either DMSO (100%) or ethanol (80%) for 10 minutes were used as positive controls.

Real-time PCR. Total RNA was isolated using Trizol reagent (Invitrogen) and cDNA prepared from 1 μg of total RNA using Superscript III as per manufacturers' instructions (Invitrogen). Real-time PCR was performed using a Rotor-Gene 3000 (Corbett Research/Qiagen, VIC, Australia) using RT2 Real-time SYBR Green/ROX PCR master mix (Qiagen). Primer sets used in this study: *β-actin*: Fwd 5'-ttgctgacaggatgcagaag-3'; Rev 5'-aagggtgtaaaacgcagctc-3', *C/ebpa*: Fwd 5'-caagaacagcaacgagtaccg-3'; Rev 5'-gtcactggtcaactccagcac-3', *Pparg*: Fwd 5'-ttttccgaagaaccatccgatt-3'; Rev 5'-atggcattgtgagacatcccc-3', *Adipoq*: Fwd 5'-tgttcctcttaatcctgccca-3'; Rev 5'-

ccaacctgcacaagttccctt-3', *Runx2*: Fwd 5'-atgatgacactgccacctctg-3'; Rev 5'-atgaaatgcttgggaactgc-3', *Sp7*: Fwd 5'-atggcgtcctctctgcttg-3'; Rev 5'-gtccattggtgcttgagaagg-3', *Alpl*: Fwd 5'-gccttaccaactcttttgtgc-3'; Rev 5'-ggctacattggtgttgagctt-3', *Bmp2*: Fwd 5'-gggacccgctgtcttctagt-3'; Rev 5'-tcaactcaaattcgctgaggac-3', *Noggin (Nog)*: Fwd 5'-cgagcgagatcaaagggct-3'; Rev 5'-tcctcctcagcttcttgctca-3', *Ibsp*: Fwd 5'-cagtccagggaggcagtg-3'; Rev 5'-ggaaagtgtggcgttctctg-3', inhibinβ A chain (*Inhba*): Fwd 5'-tgaatgaactcatggagcagacc-3'; Rev 5'-agctggctggtcctcacag-3', inhibinβ E chain (*Inhbe*): Fwd 5'-tacctgaggatcttccgttgc-3'; Rev 5'-tccagttggagtttcacgacg-3'. Changes in gene expression were calculated relative to β-actin using the $2^{-\Delta Ct}$ method **(4)**.

Western Immunoblot. Cell lysates were prepared as previously described **(5)** and equivalent amounts of protein (50 μg) were separated on 8% SDS-PAGE gels and transferred to PVDF membranes (GE Healthcare, UK). Immunoblotting was performed with the following antibodies: phospho-Akt (Thr308), phospho-Akt (Ser473), phospho-$p70^{S6K}$ (Thr 389), phospho-IRS1 (Ser636/639), phospho-FOXO1(Thr24)/3a(Thr32), total Akt, total $p70^{S6K}$, mTOR, Rictor, Raptor (Cell Signaling Technology, MA, USA), and HSP-90 (Santa Cruz, TX, USA). Following incubation with appropriate alkaline-phosphatase conjugated secondary antibodies, membranes were developed with enhanced chemifluorescence substrate (GE Healthcare). Quantitative analysis was performed using Image Quant software (Molecular Dynamics,).

Statistical Analyses. All experiments were performed in triplicate using separate MSC harvests, and data are presented as mean ± SD of a representative experiment containing quadruplicate (osteogenic and adipogenic differentiation assay) or quintuplicate (proliferation assay) wells. Statistical analyses were performed using unpaired t-tests using Microsoft GraphPad Prism 6 (GraphPad Software, CA, USA). In all cases, $p<0.05$ was considered statistically significant.

References

1. Bentzinger CF, Romanino K, Cloetta D, Lin S, Mascarenhas JB, Oliveri F, Xia J, Casanova E, Costa CF, Brink M, Zorzato F, Hall MN, Ruegg MA 2008 Skeletal muscle-specific ablation of raptor, but not of rictor, causes metabolic changes and results in muscle dystrophy. Cell Metab **8**(5)**:**411-24.
2. Short BJ, Brouard N, Simmons PJ 2009 Prospective isolation of mesenchymal stem cells from mouse compact bone. Methods Mol Biol **482:**259-68.
3. Weber K, Bartsch U, Stocking C, Fehse B 2008 A multicolor panel of novel lentiviral "gene ontology" (LeGO) vectors for functional gene analysis. Mol Ther **16**(4)**:**698-706.
4. Livak KJ, Schmittgen TD 2001 Analysis of relative gene expression data using real-time quantitative PCR and the 2(-Delta Delta C(T)) Method. Methods **25**(4)**:**402-8.
5. Jaiswal RK, Jaiswal N, Bruder SP, Mbalaviele G, Marshak DR, Pittenger MF 2000 Adult human mesenchymal stem cell differentiation to the osteogenic or adipogenic lineage is regulated by mitogen-activated protein kinase. J Biol Chem **275**(13)**:**9645-52.

Figure 1

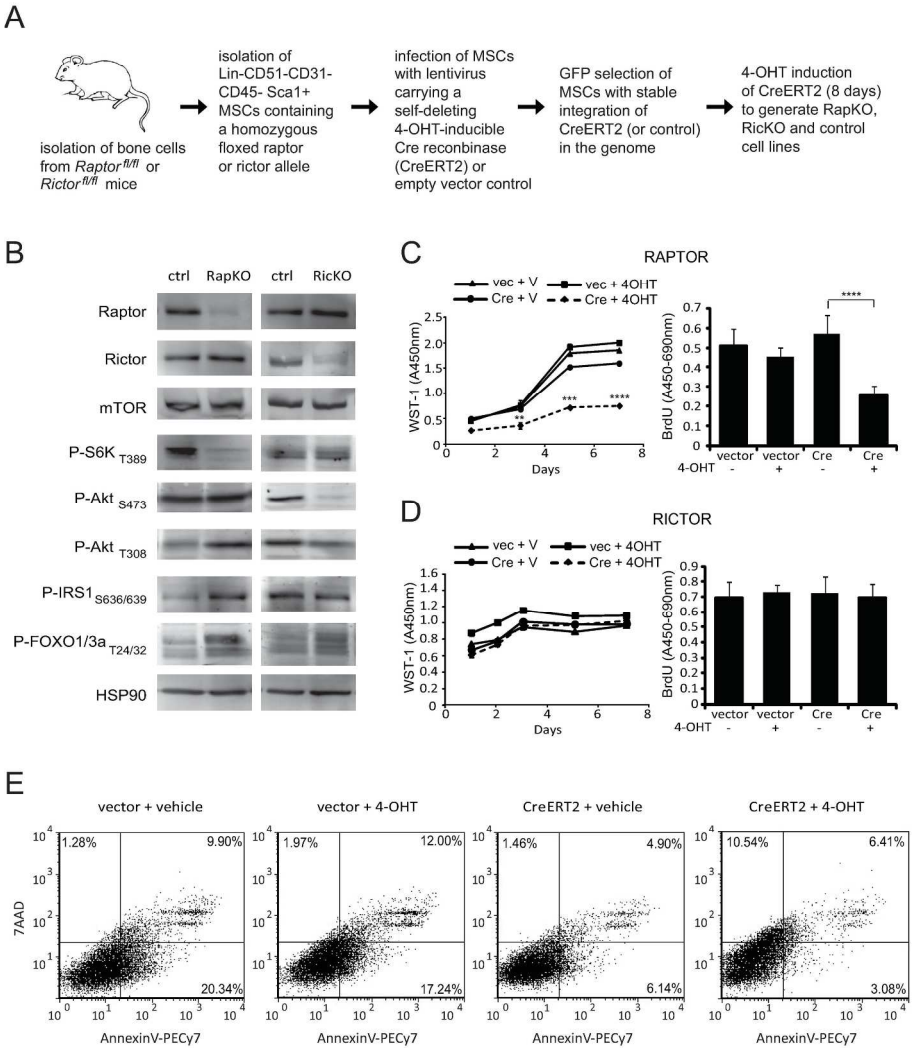

222x293mm (300 x 300 DPI)

Figure 2

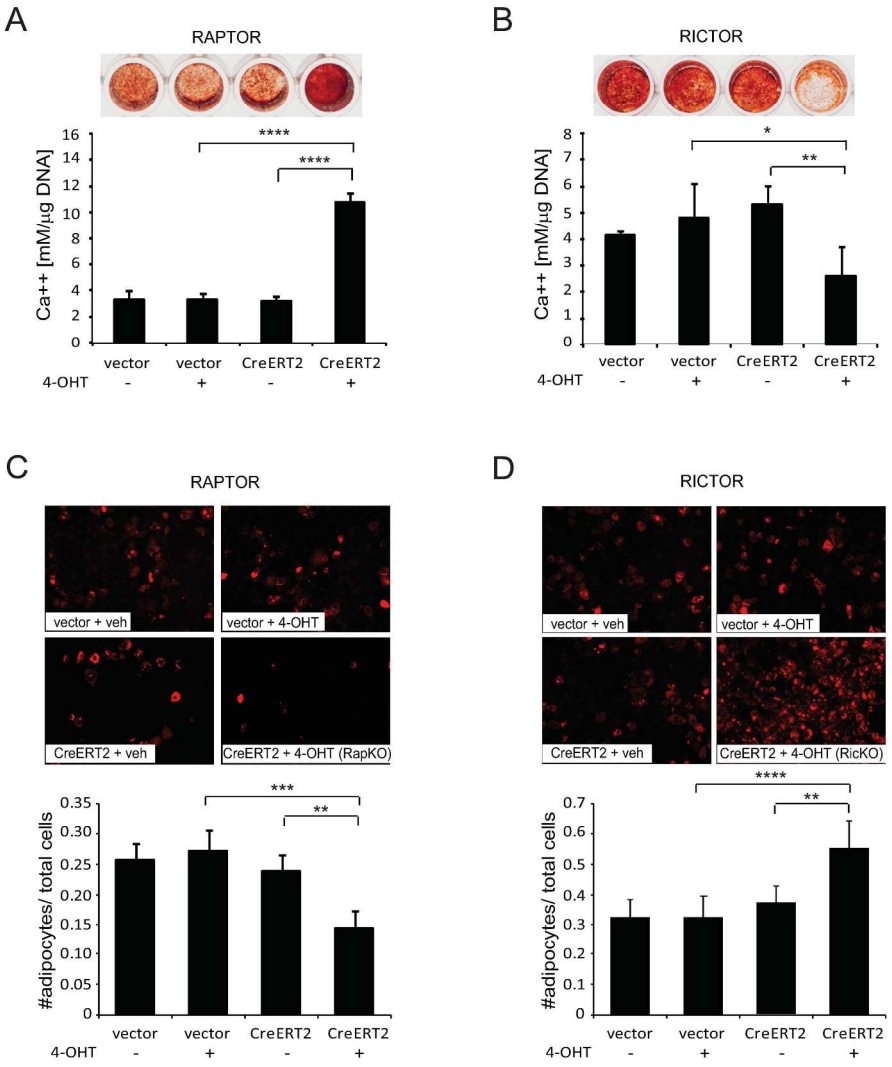

206x280mm (300 x 300 DPI)

Figure 3

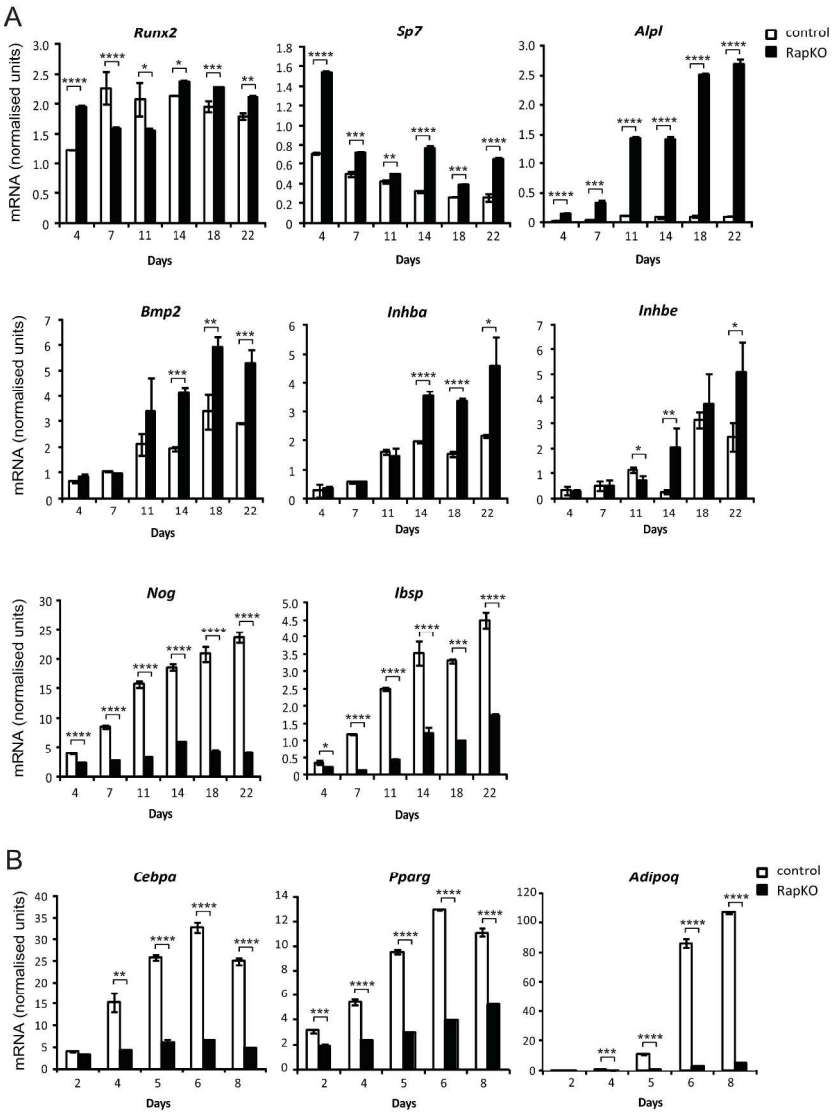

252x367mm (300 x 300 DPI)

Figure 4

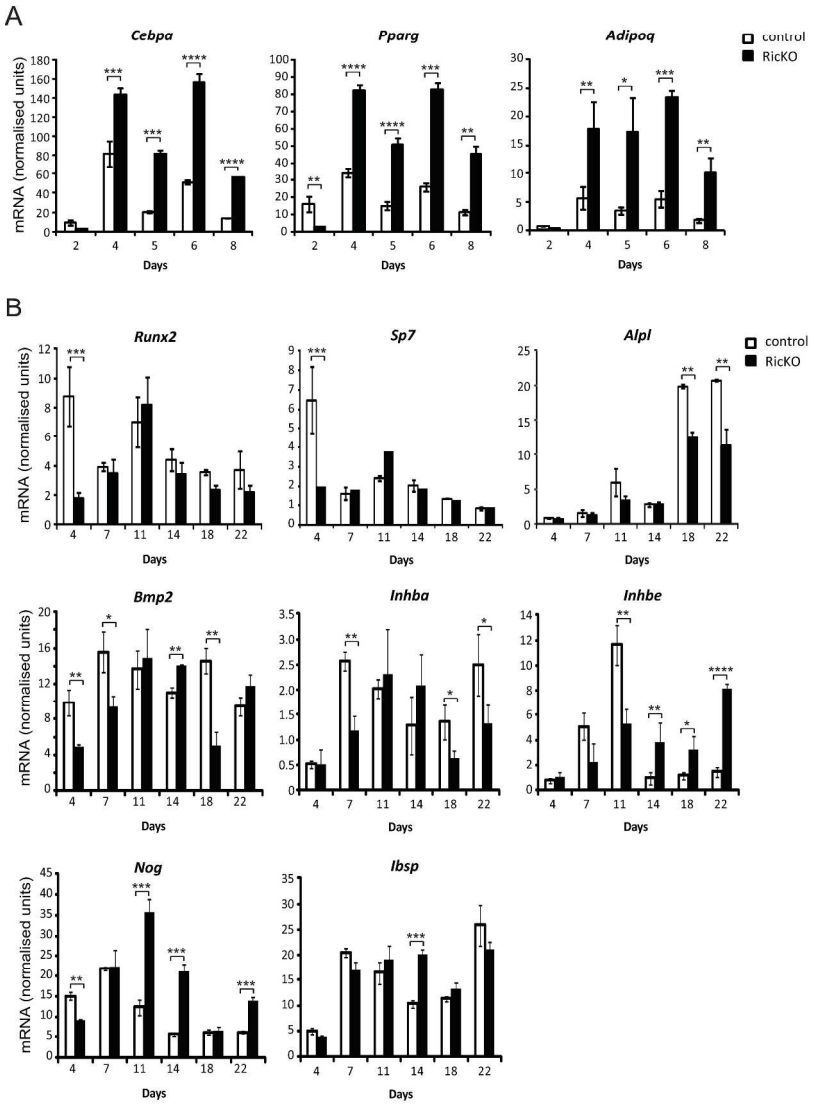

257x384mm (300 x 300 DPI)